Spatiotemporal Changes in Tornado Hazard Exposure: The Case of the Expanding Bull's-Eye Effect in Chicago, Illinois

WALKER S. ASHLEY, STEPHEN STRADER, TROY ROSENCRANTS, AND ANDREW J. KRMENEC

Meteorology Program, Department of Geography, Northern Illinois University, DeKalb, Illinois

(Manuscript received 10 July 2013, in final form 26 September 2013)

ABSTRACT

Exposure has amplified rapidly over the past half century and is one of the primary drivers of increases in disaster frequency and consequences. Previous research on exposure change detection has proven limited since the geographic units of aggregation for decennial censuses, the sole measure of accurate historical population and housing counts, vary from one census to the next. To address this shortcoming, this research produces a set of gridded population and housing data for the Chicago, Illinois, region to evaluate the concept of the ''expanding bull's-eye effect.'' This effect argues that ''targets''—people and their built environments—of geophysical hazards are enlarging as populations grow and spread. A collection of observationally derived synthetic violent tornadoes are transposed across fine-geographic-scale population and housing unit grids at different time stamps to appraise the concept. Results reveal that intensifying and expanding development is placing more people and their possessions in the potential path of tornadoes, increasing the likelihood of tornado disasters. The research demonstrates how different development morphologies lead to varying exposure rates that contribute to the unevenness of potential weather-related disasters across the landscape. In addition, the investigation appraises the viability of using a gridded framework for assessing changes in census-derived exposure data. The creation of uniformly sized grid data on a scale smaller than counties, municipalities, and conventional census geographic units addresses two of the most critical problems assessing historical changes in disaster frequencies and magnitudes—highly variable spatial units of exposure data and the mismatch between spatial scales of population/housing data and hazards.

1. Introduction

Over the past 80 years—the life span of an average American—the United States has more than doubled its population, transitioned from a rural to urban development character, and effectively escalated the exposure of its population and built environment to weather hazards. Exposure to weather extremes contains components of both vulnerability and weather hazard risk and, in a broad sense, constitutes the characteristics of the natural and/or built environment that position a system to be affected by a hazard (Morss et al. 2011). Human and engineered structure exposure has amplified rapidly throughout the United States and is arguably one of the primary drivers of increases in disaster frequency and consequences. Urban regions have continually outpaced overall national growth (Census Bureau 2012a), illustrating that weather hazard exposure landscape is not uniform or fixed, but rather is focused in specific areas and continually evolving.

The Chicago, Illinois, metropolitan area is a prime example of the enormous growth that American cities have witnessed during the twentieth and early twenty-first centuries (Auch et al. 2004; Greene and Pick 2012). The Chicago region is characterized by a dense urban core and has experienced extensive, spatially fragmented suburban and exurban growth (Theobald 2005; Greene and Pick 2013), or sprawl (Duany et al. 2000; Gillham 2002; Hall and Ashley 2008), during the last 60 years. To what extent has the growth of Chicago population and households increased exposure to weather hazards? To what degree have demographic shifts and transformations in Chicago's developed landscapes, such as that created by sprawl, led to a greater potential for a weather disasters? We assess these questions by 1) employing historical census data in a gridded framework and 2) using a portfolio of significant contemporary and synthetic tornado paths to produce a set of tornado disaster scenarios. Together, these methods are used to evaluate

Corresponding author address: Walker S. Ashley, Meteorology Program, Dept. of Geography, Northern Illinois University, Davis Hall, Rm. 118, DeKalb, IL 60115.
E-mail: washley@niu.edu

DOI: 10.1175/WCAS-D-13-00047.1

changes in potential tornado hazard impacts on the metropolitan Chicago population and its housing. Ultimately, the goal of this research is, first, to appraise a methodological framework for the spatiotemporal assessment of potential microscale disaster events and, second, to inform policy makers, emergency managers, and the public of the potential for catastrophic tornado scenarios to stimulate future mitigation strategies.

2. Background

Weather-related disasters and losses have steadily increased though time (Changnon et al. 2000; Bouwer 2011; Field et al. 2012). Uncovering and quantifying the source(s) of these trends is an area of continual dialogue and controversy in hazard assessment research (e.g., Trenberth et al. 2011; Kunkel et al. 2013), largely because of the inadequacies of current geophysical event and socioeconomic datasets (Kunkel et al. 1999; Höppe and Pielke 2006; Lerner-Lam 2007; Bouwer 2011; Kahn and Kelman 2012). However, certainties do exist—human populations continue to increase and cluster in physically vulnerable locations (Nicholls and Small 2002; Auch et al. 2004; Field et al. 2012), placing ever-increasing amounts of people and their assets in harm's way (Changnon and Burroughs 2003; Wilson and Fischetti 2010; Paulikas and Ashley 2011; Burkett and Davidson 2012). Despite decades of improvement in mitigation activities aimed at reducing impacts from extreme events (Nicholls 2001, 2011), the rapid increase in disaster losses and people affected suggests that swelling populations, development trends, and vulnerabilities are outpacing mitigation and adaptation, leading to greater disaster frequencies and amplified impacts. Through demographic and asset normalization methods, long-term, macroscale hazard impact assessments [cf. Table 1 in Bouwer (2011) and Table 3 in Barthel and Neumayer (2012)] have suggested that societal change and economic development are the primary factors responsible for the increasing trend in disaster losses (Kunkel et al. 1999; Pielke 2005; Höppe and Pielke 2006; Bouwer 2011; Barthel and Neumayer 2012; Field et al. 2012) and will likely remain at the forefront of loss attribution in the future (Pielke 2007; Barthel and Neumayer 2012; Simmons et al. 2013). However, the large-scale application of socioeconomic normalization functions used in these studies often prevents a focused appraisal of exposure changes, especially across complex spatiotemporal landscapes such as those found in metropolitan regions.

Advances in computing capabilities and software have permitted the ability of models to predict impacts of hazards using components that represent weather events, exposure rates, and measures of social and/or physical vulnerabilities (Burton 2010). Modeling research has focused most notably on hurricane, flood, and earthquake effects (e.g., Pinelli et al. 2004; Burton 2010; Dell'Acqua et al. 2013; Remo et al. 2012; Remo and Pinter 2012; Peduzzi et al. 2012), with Federal Emergency Management Agency's (FEMA's) Hazards U.S. (HAZUS; http://www.fema.gov/hazus) application allowing a spectrum of users and agencies to conduct impact loss estimations for these hazards (e.g., Scawthorn et al. 2006). Methodologies have also been developed to gauge the potential impact from microscale events, such as significant tornado events on urban locations (Rae and Stefkovich 2000; Wurman et al. 2007, hereafter WUR). These investigations transpose historical tornado cases, or their likeness, onto contemporary spatial datasets to gauge the potential effects of a violent tornado or outbreak of tornadoes on select metropolitan areas. However, this scenario research has ignored how and where changes in exposure altered the disaster geographies of extreme weather hazards. Additional scenario work by Hall and Ashley (2008) and Paulikas and Ashley (2011) formulated methods to evaluate these spatiotemporal changes at the metropolitan scale but were limited by an inability to overcome the spatial unit variation problem (Cai et al. 2006) associated with evolving enumerations that depict census data. We plan to eliminate these methodological concerns by using a homogenized procedure for assessing and quantifying changes in finescale weather hazard exposure to populations and their housing.

3. Data and methodology

a. Population and housing grid construction

Previous research on detection of changes in hazard exposure or vulnerability has proven limited since the geographic units of aggregation for decennial censuses, the sole measure of accurate historical population and housing counts in the United States, vary from one census to the next. To address this methodological shortcoming, we produced a collection of fine-geographic-scale population and housing data for the Chicago metropolitan region by employing an areal weighting (AW), or proportionate allocation, algorithm similar to those used by the Socioeconomic Data and Applications Center (SEDAC) to develop a set of 2000 U.S. grids (SEDAC 2011) and global population grids (Deichmann et al. 2001). The AW procedure apportions a raster grid representation of population or other variable from a census-defined enumeration unit (e.g., tract or block) according to the area proportion of the census unit that the grid cell encompasses (Balk et al. 2005). The creation of uniformly sized grid data on a scale smaller than counties, municipalities, and conventional census geographic units will

TABLE 1. Mean tract (1960–2010) and block (1990–2010) size area (km^2) by individual county and all counties (total), as well as the percentage change in population (pop.) and housing units (HU) from 1970 to 2010 and 1990 to 2010.

Year	Boone	Cook	DeKalb	DuPage	Grundy	Kane	Kendall	Lake	LaSalle	McHenry	Will	Total
1960 tract	—	2.21	—	16.14	—	45.25	—	34.76	—	197.85	70.96	7.59
1970 tract	121.70	2.11	—	13.21	—	30.16	—	20.98	—	113.06	55.00	7.44
1980 tract	121.70	2.02	—	9.47	—	25.14	119.39	16.44	—	93.11	46.81	7.39
1990 tract	121.70	1.84	78.31	7.51	123.86	19.96	104.46	12.54	110.13	60.88	27.85	9.40
2000 tract	121.70	1.85	78.31	5.93	123.86	20.26	104.46	8.06	110.13	33.68	26.83	8.91
2010 tract	104.34	1.88	78.27	4.03	111.47	16.56	83.48	7.95	106.17	30.42	14.47	8.30
1990 block	0.6988	0.0474	0.6384	0.0798	0.5873	0.2162	0.5952	0.1333	0.5595	0.3456	0.2777	0.1646
2000 block	0.5291	0.0387	0.5188	0.0541	0.4797	0.1597	0.4403	0.0950	0.4999	0.2221	0.1938	0.1262
2010 block	0.4124	0.0251	0.4137	0.0501	0.2280	0.1273	0.2154	0.0762	0.4446	0.1965	0.1515	0.0910
1970–2010 pop. % change	112.9%	−5.4%	46.8%	87.9%	88.7%	105.3%	335.0%	83.8%	2.3%	176.8%	173.4%	21.0%
1990–2010 pop. % change	75.8%	1.8%	34.9%	17.3%	54.8%	62.3%	191.1%	36.2%	6.6%	68.5%	89.6%	16.0%
1970–2010 HU % change	144.7%	17.5%	102.7%	152.4%	126.4%	136.2%	418.7%	135.7%	32.7%	219.8%	223.9%	47.4%
1990–2010 HU % change	74.0%	7.8%	50.2%	21.8%	58.0%	63.3%	193.3%	42.0%	14.0%	75.9%	93.3%	20.5%

address two of the most critical problems we have in assessing historical changes in disaster frequencies and magnitudes: 1) highly variable spatial units of exposure data and 2) the mismatch between spatial scales of population/housing data and weather hazards. Previous research (Schlossberg 2003) suggests that small area interpolation is best served by using the smallest census areal unit available and that the AW method is superior to other procedures for extracting data under a buffer, neighborhood boundary, or similar administrative overlay. Dasymetric mapping, which applies ancillary information (e.g., land use/cover data) to inform the areal estimation and interpolation of attributes such as population or housing units, is also suggested in the literature (Holt et al. 2004; Mennis 2009). Although arguably superior for appraising demographic attributes (Wu et al. 2005), it suffers from illogical stationarity when, for example, only one time stamp of ancillary data is available for informing a model that is being used in multiperiod change detection. Unfortunately, consistent ancillary data to inform dasymetric estimation of population and housing units for our series of time stamps do not exist.

Initially, census block boundary information for 1990, 2000, and 2010 was acquired from the University of Minnesota's National Historical Geographic Information System (NHGIS); 1990 is chosen as the initial year since this was the first census for which the block unit—the smallest geographic entity for which the Census Bureau presents data—was available. We evaluate 11 counties (Table 1, Fig. 1) in the northeast Illinois region; these counties were chosen to represent the full spectrum of development (or lack thereof) character found in the area. A grid resolution of 0.16 km^2 was used for the AW procedure at the block level; this resolution represents the mean size of all blocks in the region for 1990, which is the initial time stamp of analysis and the coarsest of the three analysis iterations. Population and housing count data at the block level were obtained from the Census Summary File 1 (SF1) archives at NHGIS for each of the three censuses. Boundary and demographic attribute datasets were conflated in a geographic information system (GIS).

In constructing the grids in the GIS, a "fishnet" at each resolution was constructed for the area of interest on an Albers equal-area conic projection. Population and housing counts at the block level were transformed from their native irregular geographic units by proportionally allocating to the grid. If a hypothetical grid cell contains 50% of the area of one census block and 20% of the area of a second census block, the housing count for that grid cell will be 50% of the housing count of the first census block and 20% of the housing count of the second census block (SEDAC 2011).

To evaluate long-term changes in potential hazard exposure for Chicago, we also assess census tract population data for two counties in the region: Cook, which is representative of an urban core, and Kane, which is typified by recent suburban/exurban development character (Greene and Pick 2012). Tracts are larger enumerations in comparison to blocks (Table 1) and, consequently, employing the AW method on a coarser grid is required. The use of tract data promotes a more informed temporal perspective of any hazard scenario research at the cost of reduced spatial resolution. We constructed population grids at 2.21 km^2 resolution for

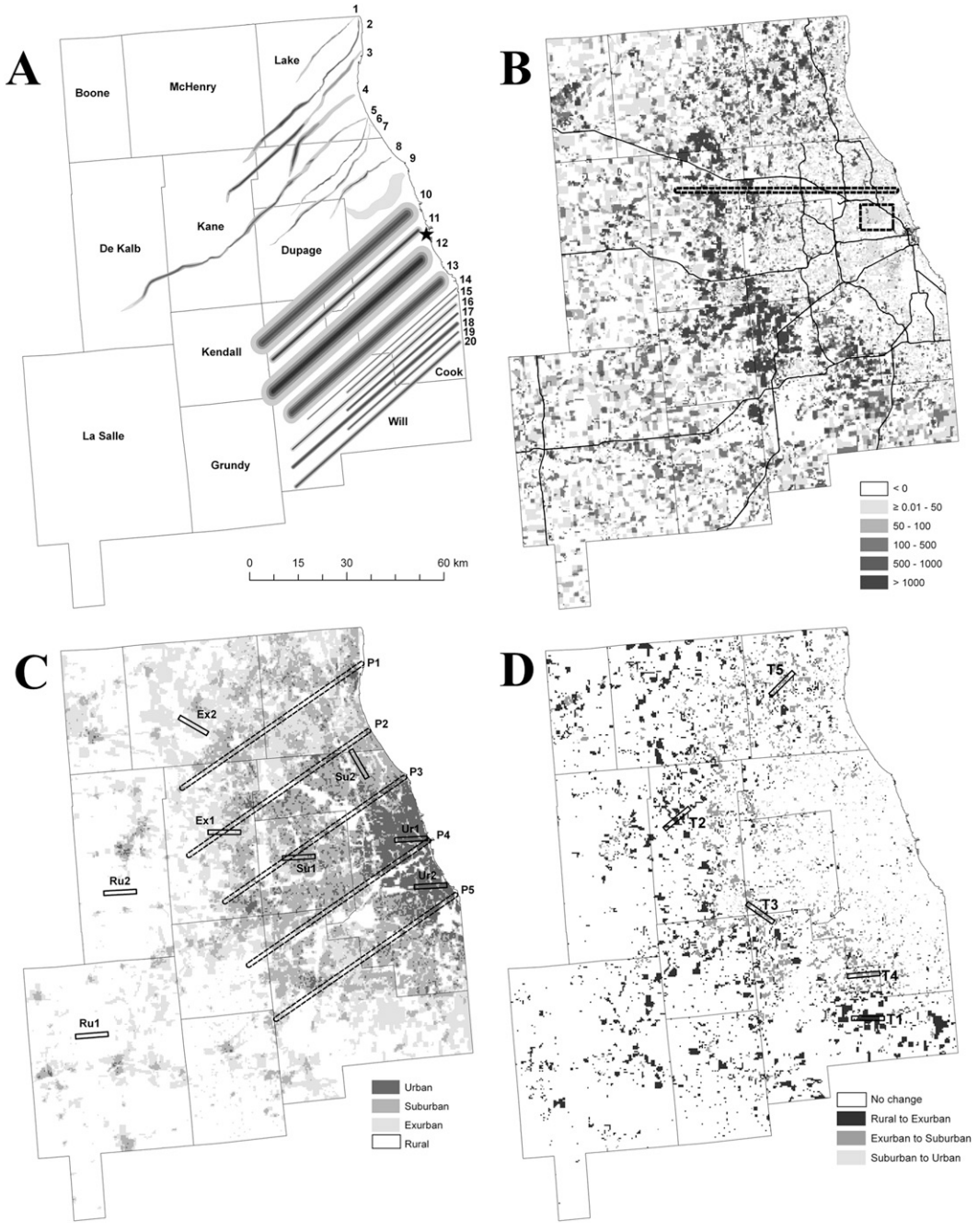

FIG. 1. (a) The Chicago-area counties under investigation in this research with historical and synthetic tracks placed across the study area. The Chicago central business district, or "The Loop," is denoted by a star. The tornado paths and numeral labels correspond to the track information found in Table 2. (b) The percentage change in population from 1990 to 2010 for each 0.16 km^2 grid cell, with 10-km-long tornado segment (cf. section 4a; width attribute derived from WUR Hybrid, or path 10 in Table 2) and scenario path S2 placed across northern Kane and Cook Counties (cf. section 4b). (c) The 2010 land-use classification based on Theobald (2005) housing density criteria, with five full-length scenario (S2) paths placed across the developed core of the study area [cf. section 4d(1)]. Eight 10-km-long S2 segments—two for each land-use type—are also placed on the map, with Ru corresponding to rural, Ex to exurban, Su to suburban, and Ur to urban [cf. section 4d(2)]. (d) The land-use change for the study area from 1990 to 2010 for three transformations assessed; white cells indicate no change or (less common) reversal of land use (urban to suburban). Five 10-km S2 segments are placed across areas that experienced notable land-use transformation, with T1 and T2 assessing rural to exurban change and T3, T4, and T5 evaluating exurban to suburban change [cf. section 4d(2)].

TABLE 2. Tornado parameters and attributes from 1) violent events from 1990, 1999, 2011, and 2013, 2) WUR synthetics, and 3) our synthetics [i.e., Ashley et al. (ASH)], which are based on mean length (km) and width (m) information gathered from all U.S. violent tornadoes from 1995 to 2011 that contained information on those elements. Area (km^2) swept out by each tornado's reported (Enhanced) Fujita-scale class is provided.

Path	Date	Min-Max F/EF scale	Fatalities	Path length	Max width	F/EF0 area	F/EF1 area	F/EF2 area	F/EF3 area	F/EF4 area	F/EF5 area	Total area
Tornado event												
1) Plainfield, IL	28 Aug 1990	F1-F5	29	26.4	548	—	8.57	2.57	0.44	0.12	0.02	11.72
2) Bridgecreek–Moore, OK	3 May 1999	F1-F5	36	61	1609	—	18.11	12.31	12.70	5.51	0.87	49.50
3) Mulhall, OK	3 May 1999	F1-F4	2	63	1609	—	31.00	17.36	6.41	12.64	—	67.41
4) Joplin, MO (NWS)	22 May 2011	EF1-EF5	158	35	1463	—	28.71	9.58	3.85	2.22	1.34	45.70
5) El Reno, OK	24 May 2011	EF0-EF5	9	101	1609	24.65	32.63	21.83	17.06	2.55	0.42	99.14
6) Washington–Goldsby, OK	24 May 2011	EF0-EF4	0	37	805	3.58	3.43	3.16	2.21	0.70	—	13.08
7) Chickasha–Newcastle, OK	24 May 2011	EF0-EF4	1	53	805	8.06	10.17	5.12	2.68	1.12	—	27.15
8) Newcastle–Moore, OK	20 May 2013	EF0-EF5	23	27	1737	11.88	5.45	2.57	1.90	1.38	0.12	23.30
9) El Reno, OK	30 May 2013	EF0-EF3	9	26	4184	—	—	—	—	—	—	73.06
Wurman et al. (WUR) synthetics												
10) Mulhall, OK (MH)	3 May 1999	F1-F4	—	60	7050	—	225.33	91.05	99.79	45.87	—	462.03
11) Bridgecreek/Moore, OK (BC)	3 May 1999	F1-F5	—	60	2315	—	65.02	27.44	20.09	11.28	19.28	143.11
12) Hybrid (HB)	—	F1-F5	—	60	8800	—	235.19	105.40	73.59	36.88	72.70	523.76
13) Hybrid Reduced (HR)	—	F1-F4	—	60	6580	—	174.85	73.47	75.32	61.80	—	385.45
14) Small (SM)	—	F1-F3	—	60	548	—	13.07	9.97	7.34	—	—	30.38
Ashley et al. (ASH) synthetics												
15) Synthetic 1 (S1)	—	EF0-EF5	—	45.21	873	20.63	4.36	4.22	5.06	4.37	1.44	40.09
16) Synthetic 2 (S2)	—	EF0-EF5	—	67.3	1390	49.72	9.57	9.99	12.00	10.37	3.41	95.06
17) Synthetic 3 (S3)	—	EF1-EF5	—	45.21	873	—	9.04	8.71	10.42	8.97	2.95	40.09
18) Synthetic 4 (S4)	—	EF1-EF5	—	67.3	1390	—	21.46	20.66	24.71	21.25	6.98	95.06
19) Synthetic 5 (S5)	—	EF1-EF5	—	45.21	873	—	14.75	8.97	8.33	5.01	3.03	40.09
20) Synthetic 6 (S6)	—	EF1-EF5	—	67.3	1390	—	34.99	21.26	19.75	11.87	7.18	95.06

Cook County and at 19.96 km^2 for Kane County. These resolutions were chosen since they were the mean size of the tracts during the first year of our tract-level analysis (1960 for Cook and 1990 for Kane).

b. *Historical and synthetic tornado tracks*

Since 1950, long-track, significant (≥8 km and ≥EF2; EF is the Enhanced Fujita scale) tornadoes have produced 85% of fatalities and 75% of reported damage; infrequent violent (≥EF4) events have been the cause of over two-thirds of all tornado deaths (Ashley 2007; Simmons and Sutter 2011). Thus, in scenario-based research and in resulting mitigation actions, it is imperative to focus on these relatively rare events. Improvements in data collection practices associated with post-hazard-event surveying (e.g., Speheger et al. 2002; Yuan et al. 2002) have generated a portfolio of hazard cartographies to utilize in hypothetical scenario assessments. In particular, extreme tornado events in the past few years have been surveyed by the National Weather Service (NWS), National Institute of Standards and Technology, Federal Emergency Management Agency, private meteorologists (e.g., Marshall et al. 2012), etc., supplying GIS-ready maps illustrating damage path attributes and, in some cases, detailed structure damage information.

Initially we gathered GIS-ready tornado paths that contain damage attribute information [Fujita (F) or Enhanced Fujita scale; Doswell et al. 2009] for contemporary, high-end tornado events (Table 2). In addition, we constructed two sets of synthetic paths that included 1) parameters and track widths constructed from 3 May 1999 mobile Doppler radar data and postevent analysis (cf. WUR) and 2) mean length and width dimensions of recorded violent (EF4 and EF5) tornadoes from 1995 to 2011 (Table 3) in conjunction with the percentage area of each EF-scale damage class swept out by the 22 May 2011 Joplin, Missouri, tornado.

The Joplin tornado is the prototypical tornado case to employ in our synthetic research since it 1) was the deadliest (158 direct fatalities) U.S. tornado since 1947 and 2) is a contemporary representation of a catastrophic tornado scenario in a densely settled area. In constructing

TABLE 3. Mean length (km) and width (m) attributes by damage class for 1995–2011 U.S. tornadoes.

F/EF damage	Count	Mean length	Mean width
F/EF0	13 232	1.90	45.43
F/EF1	5830	6.28	127.41
F/EF2	1747	13.18	286.88
F/EF3	506	26.84	568.84
F/EF4	115	42.72	815.07
F/EF5	13	67.30	1389.89
Total (F/EF0+)	21 443	4.85	104.68
Significant (F/EF2+)	2381	17.81	378.34
Violent (F/EF4+)	128	45.21	873.45

our synthetics, we used two sources of damage path information from the Joplin event: 1) the NWS's assessment (http://www.crh.noaa.gov/sgf/?n=event_2011may22_tornadotracks) and 2) aerial and structure-by-structure ground surveys conducted by Marshall et al. (2012). Dual damage path sources were used to illustrate and evaluate the differences in findings that can be found by two surveys of the same event (Fig. 2). In both cases, we focused specifically on the 10-km portion of the track that went through the settled areas of Joplin (from Schifferdecker Ave. to the west to South Kenser Ct. to the east) as this is most representative of a tornado striking a developed region. Since the damage isopleths in the NWS and Marshall et al. (2012) surveys were EF1+, we constructed an EF0 contour to represent the totality of the tornado that was based on the tornado width officially reported in NOAA's *Storm Data* (i.e., 1463 m). Comparisons (not shown) with the EF0 contour generated with Marshall et al.'s damage indicators suggest that this width corresponds with the size of the hazard as it traversed South Joplin. We fit this contour to the Marshall et al. path since this will be our primary synthetic path tool of assessment. The area swept out by each damage class was then converted to a percentage of the total 10-km track segment (Table 4) to promote synthetic tornado path construction (Fig. 2).

c. *Path and grid intersect*

To evaluate changes in tornado exposure and assess "worst case" (Clarke 2005) tornado scenarios for Chicago, we conflated the exposure attribute grids with our tornado path portfolio in a GIS. In this step, we used the underlying census attribute grid (population or housing unit) and placed a single tornado path, or path segment, over a desired location. Path placement was not random; the paths were placed purposely over areas to evaluate how changing development patterns influence the potential tornado disaster landscape. As in Hall and Ashley (2008), we assess specifically areas that have experienced a considerable increase in development due to sprawl. Similar to Rae and Stefkovich (2000) and WUR, but using both temporal and spatial perspectives, we evaluate how the evolving demographics of urban cores have influenced worst-case scenarios. Finally, we examine changes in rural and exurban development characteristics in the Chicago region. The goal of this analysis was not to produce a comprehensive inventory of all possible scenarios for the area; rather, we focus on specific development characters and changes in those landscapes to reveal how disaster consequences may be amplified by exposure.

Once the path is overlaid on the exposure attribute grid, we "intersect" the demographic grid and tornado path layers in the GIS to combine the geospatial data into a single layer that retains both field and boundary data. Thereafter, we used a "dissolve" tool to generate attributes for each year considered (e.g., population affected by a specific damage rating for scenario in 1990) that may be used in subsequent analysis. In overlaying their block-level attribute data with the 1990 Plainfield tornado path, Hall and Ashley (2008) employed the "intersecting" method (Schlossberg 2003). This procedure generates the total number affected by the hazard by summing the attribute values for all blocks that are within or intersect the tornado path, even if the path clipped merely a small proportion of the block enumeration. This methodology leads to overestimation of those affected (Schlossberg 2003; Hall and Ashley 2008). Conversely, in our calculation approach, we use the AW method to produce a more accurate representation of the number of people potentially affected. Specifically, along the edges of the tornado and EF classes, where the track/classes will transect only parts of a grid cell, we use the AW procedure to adjust tallies of population and/or housing based on the fraction of the grid cell impacted.

The scenario tallies of affected people are estimates based on places of residence, since census population data are based on number of residents in an enumeration area. While the number of people affected may vary depending on the situation, the number of housing units impacted should be a relatively robust marker for assessing spatiotemporal changes in disaster potential landscape.

4. Results

The results of this research are presented in four parts. First, we demonstrate the methodological framework used to measure changes in residential exposure to high-end, microscale hazards such as violent tornadoes. Exposure is assessed under three event scenarios: the previous synthetic worst-case scenario, contemporary violent events, and our own synthetic path constructions. Second, we address the implications of downscaling

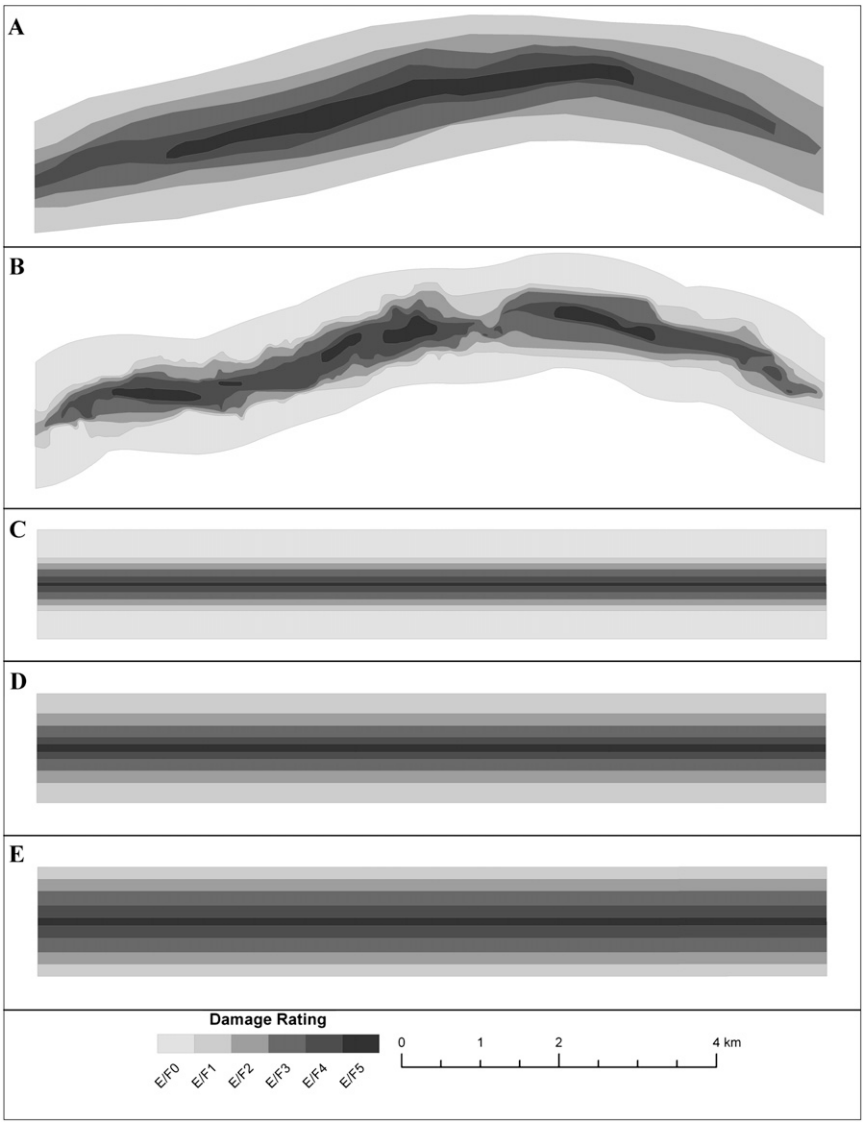

FIG. 2. (a) The NWS survey assessment for the 2011 Joplin EF5 tornado; (b) the Marshall et al. survey assessment for the Joplin tornado; (c) the Synthetic 2 (EF0-EF5) tornado path based on the Marshall et al. Joplin survey and 1995–2011 mean tornado path length/width; (d) the Synthetic 6 (EF1-EF5) tornado path based on the NWS Joplin Survey and 1995–2011 mean tornado path length/width; and (e) the Synthetic 4 (EF1-EF5) tornado path based on the Marshal et al. Joplin survey and 1995–2011 mean tornado path length/width.

demographic data from alternative enumeration geography (county or tract versus block level). In the last sections, we calculate the spatiotemporal changes in exposure consequences to potential violent tornadoes across the Chicago region to discover how the disaster landscape has evolved across time and differing development settings.

a. Comparison of path attributes

The areal extent of tornado damage is controlled by basic length and width dimensions of the hazard, whereas the damage magnitude is related to tornado core wind speed and modulated by construction practices, the age and quality of structures affected, the length of time a structure is affected by the tornado, and, in the case of events that cross over areas devoid of engineered structures, the lack of viable damage indicators that can result in inaccurate assessments of intensity (McDonald and Mehta 2006; WUR). Before performing any scenario-based research, including that which may be considered worst-case (Clarke 2005; WUR), it is important to evaluate the validity of spatial and intensity attributes of tornado events that may be used to model potential

TABLE 4. The area (km^2) and proportion of each EF damage class for the 10-km segment of the Joplin tornado that impacted the developed areas of the city.

	Marshall et al. (2012) EF0-EF5		Marshall et al. (2012) EF1-EF5		NWS (2011) EF1-EF5	
Damage	Area	% area of track segment	Area	% area of track segment	Area	% area of track segment
EF0	7.949	51.1	—	—	—	—
EF1	1.695	10.9	1.695	22.3	6.368	36.44
EF2	1.645	10.57	1.645	21.62	3.904	22.35
EF3	1.982	12.74	1.982	26.05	3.652	20.91
EF4	1.719	11.05	1.719	22.58	2.206	12.63
EF5	0.567	3.64	0.567	7.45	1.339	7.67
Total	15.557	100	7.608	100	17.469	100

disaster circumstances. As argued by Brooks et al. (2008), it is important to provide emergency managers and planners with an assessment of realistic high-end events so that they are not overwhelmed by casualty and damage estimates and, possibly, disregard disaster prospects.

Of the roughly 1500 tornadoes that occur each year in the United States, less than 0.6% (or approximately 9 yr^{-1}) are rated violent (Table 3). While intensity (as inferred by the EF scale) of tornadoes cannot be correlated explicitly with length or width, there is evidence that, generally, both path length and width tend to increase with increasing F/EF scale (Brooks 2004). The mean length (width) of violent tornadoes is much longer (wider) than all tornadoes as well as significant tornadoes (Table 3). The mean area theoretically swept out (length × maximum width) by a violent tornado is 39.46 km^2, whereas tornadoes across all (significant) damage classes were a modest 0.51 km^2 (6.74 km^2). Therefore, based on contemporary tornadoes, violent events have theoretical damage footprints that are over 5 times the size of all significant tornadoes and nearly 80 times the size of all documented tornadoes. Logically, the larger the area swept out by the core flow of a tornado, the greater the likelihood that casualties and damage to the built environment will occur.

There were 144 recorded tornadoes from January 1950 to June 2012 with path widths greater than 1.76 km (1 mi) with only three events reported wider than 3.5 km (2 mi), including 22 May 2004 Hallam, Nebraska, F4 (4.4 km, 2.5 mi; McCarthy and Schaefer 2005); 4 May 2007 Hopewell, Kansas, EF3 (3.9 km, 2.2 mi; Lemon and Umscheid 2008); and 7 June 2008 Pardeeville-Cambria, Wisconsin, EF2 (3.52 km, 2 mi) (Fig. 3). Two Oklahoma tornadoes in May 2013 provide additional, contemporary evidence of extremely wide cases. The Newcastle-Moore, Oklahoma, tornado of 20 May 2013 was over

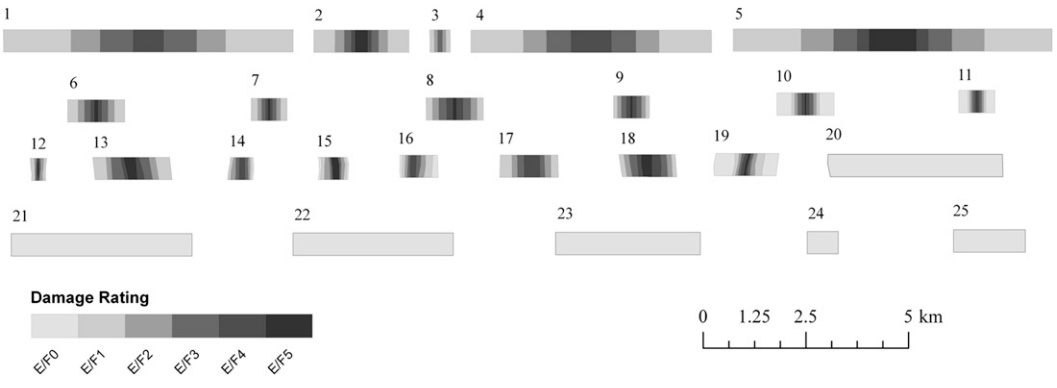

FIG. 3. Tornado and damage: intensity widths for the observed and synthetically derived events in Table 2. The segments for observed tornadoes represented were selected by subjectively determining where the tornado was at its widest during its most intense (as inferred by F/EF scale) phase. Numbers correspond to 1) WUR Mulhall, OK (MH), 2) WUR Bridgecreek/Moore (BC), 3) WUR Small (SM), 4) WUR Hybrid Reduced (HR), 5) WUR Hybrid (HB), 6) ASH Synthetic 6 (S6), 7) ASH Synthetic 5 (S5), 8) ASH Synthetic 4 (S4), 9) ASH Synthetic 3 (S3), 10) ASH Synthetic 2 (S2), 11) ASH Synthetic 1 (S1), 12) Plainfield, IL, 13) Joplin, MO (NWS), 14) Washington–Goldsby, OK, 15) El Reno, OK (2011), 16) Chickasha–Blanchard–Newcastle, OK, 17) Mulhall, OK, 18) Bridgecreek/Moore, OK (1999), 19) Newcastle–Moore, OK (2013), 20) El Reno, OK (2013) EF3, 21) 22 May 2004 Hallam, NE F4, 22) 4 May 2007 Hopewell, KS EF3, 23) 7 Jun 2008 Pardeeville–Cambria, WI EF3, 24) mean significant (F/EF2+) events from 1995–2011 (Table 3), and 25) mean violent (F/EF4+) from 1995–2011.

1.7 km wide and the El Reno, Oklahoma, tornado of 30 May 2013 was assessed at nearly 4.2 km wide, surpassing the 2004 Hallam, Nebraska, event as the widest tornado recorded. The mean width of contemporary significant (violent) tornadoes is less than 0.4 km (0.9 km), illustrating that the synthetic tornadoes and affiliated impact tallies generated by WUR may not be "realistic high-end cases" as suggested by Brooks et al. (2008) (Tables 2 and 3, Fig. 3). The WUR "observation-constrained model" synthetics were generated using 1) observed Doppler on Wheels (DOW) wind speed and size attributes at the time of maximum DOW-observed intensity for the 3 May 1999 Mulhall and Bridgecreek/Moore tornado events and 2) hypothetical cases that were representative of the worst of the tornado size/magnitude characteristics from the remotely sensed, DOW-derived attributes of these events (Table 2). Specifically, the path widths of three of the five synthetics used by WUR—that is, the 6.6-km-wide Hybrid Reduced (HR), 7.1-km-wide Mulhall (MH), or 8.8-km-wide Hybrid (HB)—are between 50% and 100% wider than the widest tornadoes ever recorded, the 2004 Hallam F4 and the 2013 El Reno EF3. The EF0+ path widths of the WUR tornadoes could be considerably wider than the reported values in WUR's Table 1 since the diameters stated in their study only included winds greater than 43 m s^{-1}, which is equivalent to the midrange of an F/EF1 (the F1 range includes estimated three second gusts of 35–52 m s^{-1}, whereas the EF1 spans 38–49 m s^{-1}). In the most extreme synthetic, the area swept out by ≥43 m s^{-1}, or EF1, winds is over 500 km^2, or almost the entire size of the city of Chicago (588 km^2). While there is historical precedent for extreme long-track events with over 30 events surpassing reported lengths of over 200 km since 1950, there is considerable discrepancy in the extreme width attributes found in the reported tornado record and WUR synthetics. Brooks et al. (2008) and Blumenfeld (2008) document concerns with the probability of death values used by WUR; however, our comparison of reported and derived tornado widths suggest that at least part of the extreme impact tallies found in the WUR study may be due to the improbable tornado widths. This dimensional argument suggests that the area, residents, housing units, and death estimates found in WUR's scenarios may not be plausible even in "hyper-worst case" situations.

We evaluated the tornado width characteristics found in Table 2 and illustrated in Fig. 3 by transposing each scenario onto a high-density, single-family housing area that typifies the developed landscape outside the Chicago central business district (CBD). Specifically, each of the path segments was constrained by a 10-km length, whereas the width was determined by the maximum F/EF0 or F/EF1 width attribute in Table 2. The 10-km length approximates the worst portion of the 2011 Joplin EF5 tornado segment that directly affected the developed area of the city (Figs. 1b and 2). Thereafter, we centered each tornado segment over the intersection of Diversey and Laramie Avenues in Chicago's northwest side, calculating the area, 2010 population, and number of 2010 housing units and households affected in each scenario. The results highlight the dichotomy between WUR tornado scenarios and observed cases or scenario events based on the 2011 Joplin EF5 (Table 5). For example, the WUR HR, MH, and HB scenarios affect nearly 3.5 to 4.5 times the area of the "worst of" observed 2011 Joplin segments, even when length is restricted. The increase in area affected in these WUR scenarios leads to subsequent amplification of population (2.1–2.7 times the number of people compared to Joplin scenario), housing units (2.8–3.7 times), and households (2.8–3.6 times) impacted. The 31 May 2013 El Reno tornado was over 3 times the size of the Joplin event, suggesting that this recent case may provide the most realistic high-end width attribute to be employed in scenario work. In comparison, WUR HB, MH, and HR scenarios all affect areas 1.3 to 1.8 times larger than this modern width record holder. While it is possible that the widths found in WUR study could occur, they appear improbable based on even the most extreme cases found in the historical tornado record. The probability of WUR's high-end widths occurring over a high-density developed landscape such as that found in the Chicago region appears even more remote since only 2.2% of the conterminous United States was characterized as urban and/or suburban (<0.69 ha per housing unit) in 2000, rising to a forecasted 3.1% by 2020 (Theobald 2005).

b. *Comparison of data metrics*

Census attribute data are available for a spectrum of geographic entities, from blocks, block groups, and tracts at the finescale, to counties and states at the intermediate scale, to divisions, regions, and the nation at the coarse scale (Census Bureau 1994). Vulnerability analysis of relatively small spatial-scale hazards, such as tornadoes, necessitates the use of fine-resolution datasets to instruct the spatiotemporal understanding of physical exposure's culpability in weather disaster composition. Both block and tract spatial dimensions can change extensively across a geography, from very small regions in urban areas to very large regions in exurban or rural locations. For example, the mean block (tract) size of urban Cook County in 2010 is 0.0251 km^2 (1.88 km^2) and the mean block size of more rural Boone, DeKalb, or LaSalle County is over an order of magnitude larger, or, in excess of 0.41 km^2 (78–106 km^2) (Table 1). Consequently,

TABLE 5. Tornado segment impact characteristics based on a fixed 10-km length and corresponding width attributes found in Table 2, ranked from highest to lowest area impacted. The segments were centered over Diversey and Laramie Avenues on Chicago's northwest side (see Fig. 1b for region represented in WUR HB scenario).

Tornado	Area (km^2)	Population affected	Housing units affected	Households affected
WUR HB	78.13	497 226	184 921	167 168
WUR MH	70.90	456 016	168 697	152 616
WUR HR	58.92	388 177	141 853	128 627
El Reno, OK (2013)	41.58	292 241	104 088	94 230
WUR BC	23.27	184 388	65 739	59 898
Joplin, MO (NWS)	17.47	137 763	50 428	45 974
Mulhall, OK	14.29	114 679	41 270	37 743
ASH S4	13.96	111 684	40 175	36 736
ASH S2	13.96	111 734	40 185	36 746
ASH S6	13.96	111 596	40 157	36 718
Newcastle–Moore (2013)	13.70	108 692	38 513	35 204
Bridgecreek–Moore, OK	13.54	110 263	39 660	36 176
El Reno, OK (2011)	11.81	88 952	32 815	29 921
ASH S3	8.77	69 044	25 209	23 114
ASH S1	8.77	69 191	25 219	23 122
ASH S5	8.77	69 123	25 214	23 119
Chickasha, OK	8.57	70 130	24 763	22 457
WUR SM	4.97	38 368	14 124	12 976
Washington–Goldsby, OK	4.91	39 216	13 971	12 847
Plainfield, IL	4.50	34 161	12 208	11 217

the use of block-level data to inform the grids is desirable when analyzing microscale hazards, such as tornadoes, and their potential impacts. Unfortunately, block- and block-group-level data were first available in 1990, and only complete at that scale for the entire United States in 2010. Tract-level data exist for some counties in metropolitan statistical areas (MSAs) for a longer record, but data availability is restricted largely to those counties that constituted or are near the urban core. How do these different scales of census enumeration units affect the AW-gridded downscale exposure tallies[1] and, ultimately, conclusions?

To evaluate this scale issue, we positioned synthetic tornado track 2 (S2; Table 2, Fig. 1b) across the northern portions of Cook and Kane Counties and calculated the number of people hypothetically affected in this scenario for 1990, 2000, and 2010 (Table 6). We chose these two counties since Cook represents an urban area with high-resolution block and tract enumerations, whereas Kane typifies suburban and exurban development characteristics; the two counties have disparate mean block and tract enumerations (Table 1).

Results reveal a bimodal relationship between impacts by county across all data frameworks (i.e., gridded versus base census geographies, which we call "raw" data) and enumeration types (i.e., county, tract, block) for the same year (Table 6). The much larger enumerations in Kane County versus Cook lead to percentage differences that are consistently greater in Kane.

When examining variation across the gridded and raw census enumeration frameworks of analysis (Tables 6 and 7), impacted population counts and percentage differences are close except for the case of Kane tract-level analysis. Broadly, this finding confirms that downscaled gridded data can be substituted as an areal unit of measurement in scenario-based work to provide an efficient structure for assessing not only the spatial changes in impacts, but also differences found across time stamps. Appropriately scaled gridded data overcome the spatial irregularity, variation in scale, and degree of aggregation problems present in raw census data; all issues that can affect the reliability of subsequent spatiotemporal analyses. Another benefit of the gridded framework is its capability of tracking developed landscape evolution and possible scenario impacts in a consistent manner. A gridded framework also promotes the inclusion of forthcoming censuses and potential conflation of supplemental data types.

At coarser resolutions, differences between Cook gridded tract and raw census tract population are much less than those of Kane for all years. While gridded block to census block population differences seem to illustrate

[1] Standard protocol for assessing accuracy and reliability of modeled data is to compare those data against "truth" data. In the absence of truth data, we are limited to assessing consistency by comparing source data at standard census enumerations. Ideally, we would verify the modeled data against finer-scale Census data. Unfortunately, the Census is unable to conduct special tabulations based on geographic coordinates, or for user-defined areas smaller than blocks.

TABLE 6. Population affected in northern Cook and Kane Counties from a hypothetical tornado (scenario S2; Table 1 and Fig. 1b) in 1990, 2000, and 2010. Percentage differences of the counts for the differing enumerations used to construct the grids (block and tract) and the counts generated by using county attribute density are provided, including county to tract, tract to block, and county to block. For instance, in the grid-to-grid enumeration or raw-to-raw enumeration comparisons, if the percent difference is positive it would indicate that *more* people were affected hypothetically by the tornado in the larger (County) resolution than the finer (Tract). Comparisons of tallies generated by using irregular census enumerations vs the gridded framework are also shown.

		Grid comparison			Census enumeration comparison			Grid to census enumeration comparison	
Population									
County Name	Year	County	Tract	Block	County	Tract	Block		
Cook	1990	139 647	124 010	124 331	139 647	124 906	124 388		
	2000	147 078	134 877	136 347	147 078	134 901	136 684		
	2010	142 098	134 840	135 531	142 098	134 983	135 814		
Kane	1990	6357	11 498	20 876	6357	20 222	21 201		
	2000	8092	13 381	22 997	8092	22 888	23 335		
	2010	10 318	15 131	23 125	10 318	24 337	23 465		
Pop. difference									
County name	Year	County to tract	Tract to block	County to block	County to tract	Tract to block	County to block	Gridded tract to census tract	Gridded block to census block
Cook	1990	15 636	320	15 316	14 741	517	15 258	895	58
	2000	12 201	1470	10 731	12 177	1783	10 394	24	337
	2010	7258	691	6567	7115	831	6284	142	283
Kane	1990	5141	9379	14 519	13 865	979	14 844	8724	325
	2000	5289	9616	14 905	14 796	447	15 243	9507	338
	2010	4813	7995	12 808	14 019	872	13 147	9206	339
% difference									
County name	Year	County to tract	Tract to block	County to block	County to tract	Tract to block	County to block	Gridded tract to census tract	Gridded block to census block
Cook	1990	11.9	−0.3	11.6	11.1	0.4	11.6	−0.7	0.0
	2000	8.7	−1.1	7.6	8.6	−1.3	7.3	0.0	−0.2
	2010	5.2	−0.5	4.7	5.1	−0.6	4.5	−0.1	−0.2
Kane	1990	−57.6	−57.9	−106.6	−104.3	−4.7	−107.7	−55.0	−1.5
	2000	−49.3	−52.9	−95.9	−95.5	−1.9	−97.0	−52.4	−1.5
	2010	−37.8	−41.8	−76.6	−80.9	3.6	−77.8	−46.7	−1.5

less difference, the much larger tract size in Kane (Table 1) leads to variation in population estimates that are greater than those of Cook. These results indicate that finescale hazard scenario studies based on tract-level data may be reliable for areas with consistently high population densities (e.g., Cook County) because of their finer enumeration sizes and consistency among areal units. However, scenario investigations using raw or gridded data based on tract-level geography in more sparsely populated areas, or regions that have undergone substantial development during the period under investigation, will be less reliable due to their large and spatiotemporally varying enumerations. Population impact count extractions based on county-level data are the poorest areal unit of measurement appraised as illustrated by the consistent large percentage differences found in the county versus tract and block for both gridded and raw frameworks. A variation-range matrix (Table 7) confirms that the use of county data can lead to large count and percentage differences, suggesting that the use of county-level demographic data to gauge sub-county-level, microscale hazard impacts can lead to inaccurate conclusions. In summary, no matter how one estimates exposure attributes, there is always potential error—but that error is far less when attribute information is more closely matched to the scale of the event.

c. *Macroscale changes in Chicago exposure*

To understand how tornado disaster potential has evolved, it is necessary to appreciate the character and trends of land-use dynamics through time and how those development patterns contribute to changes in exposure. Chicago has experienced a dramatic growth with a shift of population from the old industrial suburbs to the regions' new economy suburbs (Greene and Pick 2012, 2013). This pattern of expansion has led to decentralization of people and a metropolitan region with a polycentric quality—that is, it has multiple downtowns, with many of those ''new'' downtowns in edge cities (Greene and Pick 2012). This development pattern is

TABLE 7. The resulting affected populations for varying enumeration metrics based on S2 scenarios placed over the same location highlighted in Table 6 and Fig. 1b for 2010. The percent difference, or change, in the counts from 1990 to 2010, as well as associated ranges between enumerations, are provided.

1990	Raw	AW	Variation (+/−)
County	28 721	28 721	—
Tract	96 776	94 942	1835
Block	98 787	98 112	674
Variation (+/−)	−70 066	−69 391	
2010	Raw	AW	Variation (+/−)
County	29 225	29 225	—
Tract	110 079	108 212	1867
Block	112 701	111 734	967
Variation (+/−)	−83 475	−82 509	
1990–2010	Raw	AW	Range (+/−)
County	1.76	1.76	—
Tract	13.75	13.98	−0.23
Block	14.08	13.88	0.20
Range (+/−)	−12.33	−12.13	

dominated by sprawl, which leads to an ''expanding bull's-eye effect.'' This effect argues that targets—that is, humans and their possessions—of geophysical hazards are enlarging as populations grow and spread. Consequently, it is not solely the population magnitude that is important in creating disaster potential; rather, it is how the population, and its affiliated built environment, is distributed across space that determines how the underlying disaster components of risk and vulnerability are realized.

The total population for our study area has increased from just over 7.2 million in 1970 to 8.8 million 2010, a 21% surge. Most of the population gain was witnessed in the latter two decades, signifying population growth acceleration (Table 1). The number of housing units during the 1970–2010 period swelled from 2.4 million to just over 3.5 million, an increase of nearly 47.4%. Thus, the built environment (as measured by housing units) has increased at a faster rate than the number of people. As a consequence, any amplification in tornado losses from potential tornado disasters would be greater for insured or uninsured housing damages than human casualties.

To examine the development exposure change across our study area, we employed Theobald's (2005) land use classification on the grids and, thereafter, examined the changes temporally. ''Urban'' was defined as a grid cell that contained housing densities less than 0.1 ha per unit, ''suburban'' as 0.1–0.68 ha per unit, ''exurban'' as 0.68–16.18 ha per unit, and ''rural'' as greater than 16.18 ha per unit. For the region examined in this study (Fig. 1c), the number of urban classified cells increased from 4.5% to 5% from 1990–2010, whereas the number of rural cells decreased from 58.4% to 53.1% during the same period

TABLE 8. Number of 0.16 km^2 cells, and percentage of total area, for each land use type in the 11-county Chicago region for 1990, 2000, and 2010.

	Count			% of total area sq. km			% change
Land-use type	1990	2000	2010	1990	2000	2010	1990–2010
Urban	4759	5129	5343	4.5	4.8	5.0	0.6
Suburban	14 052	16 430	19 186	13.2	15.4	18.0	4.8
Exurban	25 707	25 619	25 543	24.0	23.9	23.9	−0.2
Rural	62 622	59 962	57 068	58.4	55.9	53.1	−5.2

(Table 8). The rural–urban interface, which is characterized by suburban and exurban sprawl, witnessed a dichotomy in change by classification type. The percentage area that was categorized as suburban increased from 13.2% to 18% over the 20-yr period, resulting in the largest change (4.8%) in development type for the region. Conversely, the exurban classification changed relatively little during the same time period. These data suggest that far more land was converted to a relatively high-density sprawl mode in comparison to the low-density development that typifies exurban areas. Collectively, the potential number of hazard ''targets'' has grown in magnitude and expanded, confirming the expanding bull's-eye effect and increasing potential for disaster, at least on the scale of the metropolitan region.

d. Spatiotemporal assessment of exposure impacts for worst-case scenarios

To evaluate change in exposure to potentially catastrophic tornadoes, we employ two scenario-based approaches. The first uses a full-dimension synthetic tornado and the second uses a 10-km synthetic tornado segment. In both scenario procedures, we overlay the tracks/segments atop the block-level, AW-gridded exposure data to estimate the residents and numbers of housing units exposed to each hypothetical tornado case.

1) FULL-DIMENSION SYNTHETIC SCENARIOS

Initially, we superimpose five full-length tornado paths based on synthetic S2 across the study area, with the paths spaced north to south, 15–20 km apart, and ceasing at the Lake Michigan shoreline. The use of a synthetic path removes the methodological concern expressed by Wurman and Alexander (2005), WUR, and Wurman et al. (2008) that transposing historical events that tracked over largely rural locations (in the case of many of the tornadoes in the 3 May 1999 outbreak or the Plainfield event 28 August 1990) atop urban conglomerations [Dallas–Fort Worth in Rae and Stefkovich (2000) and Chicago suburbs in Hall and Ashley (2008)] leads to underestimation of tornado disaster potential in more dense residential areas. Wurman and Alexander (2005)

TABLE 9. Number of people and housing units affected and affiliated 1990–2010 percentage changes of total impacted for five simulated tracks of tornadoes across Chicago region based on the S2 scenario (cf. Fig. 2c). Counts for those areas affected by significant (EF2+) and violent (EF4+) damage are provided.

		Population				Housing units			
Position	Year	EF2-EF5	EF4-EF5	EF0-EF5	1990–2010 % change	EF2-EF5	EF4-EF5	EF0-EF5	1990–2010 % change
1	1990	14 155	5451	35 947		5554	2138	13 921	
	2000	19 953	7612	52 418		7167	2715	18 906	
	2010	22 292	8591	56 327	56.7%	8206	3160	20 741	49.0%
2	1990	24 790	9600	63 458		9731	3764	24 393	
	2000	25 780	9786	69 923		10 022	3802	26 765	
	2010	28 269	10 916	74 920	18.1%	11 355	4396	29 646	21.5%
3	1990	38 935	14 867	104 961		14 975	5700	40 335	
	2000	43 592	16 743	115 892		16 734	6450	43 853	
	2010	46 300	17 841	120 828	15.1%	18 013	6938	46 744	15.9%
4	1990	57 214	21 772	161 378		22 881	8505	65 782	
	2000	66 676	25 130	185 859		25 779	9477	75 043	
	2010	73 022	27 292	205 771	27.5%	32 009	11 599	95 139	44.6%
5	1990	37 411	14 240	102 587		12 857	4932	34 798	
	2000	39 278	15 090	105 294		14 048	5399	37 413	
	2010	35 461	13 624	95 105	−7.3%	13 999	5373	37 334	7.3%

and Wurman et al. (2008) argue that there can be notable differences between the EF-scale quantified damage caused by strong-to-violent winds on the observable developed landscape and the likely extent of strong-to-violent modeled surface winds based on observations from DOWs due to the lack of damage indicators in rural locations. This discrepancy surfaced in the contentious rating of the 31 May 2013 El Reno tornado. The lack of damage indicator restriction can minimize damage potential of tornadoes when historical events, and their damage-intensity patterns, are transposed to a location with dramatically different development character. Based on prior assessments, the S2 path comprises plausible ''worst case'' dimensions and magnitude attributes since it is constructed from contemporary violent tornado footprints and damage spatial characteristics from the worst segment of the Joplin EF5 path. The scenario paths were oriented from west-southwest to east-northeast, which is the dominant tornado direction mode found in a prior climatology (Suckling and Ashley 2006).

Four of the five scenarios experienced greater than double-digit percentage increases in population and housing units from 1990 to 2010 (Table 9). The only scenario that had a decrease in an exposure metric was scenario P5. This case traversed the urban south side of Chicago, a region that has witnessed a notable loss in population during this period (Greene and Pick 2012). Despite the population loss, the hypothetical tornado path affected 7.3% more housing units. This dichotomy in exposure is due to the population decrease found in the aforementioned urban region, a lack of corresponding housing unit decrease in that same area, and increases in suburbanization and exurbanization across the first half of the track. Scenario P1 had the largest increase in population (housing unit) change, with 49% (57%) increase in exposure metrics. The P1 scenario impacted the north side of Chicago, an area that has undergone some of the greatest population and housing unit increases in the region (Table 1), with most of that development falling into suburban and exurban land use types (Figs. 2c,d). Scenario P4 moved through locations consisting largely of suburban and urban development, terminating near the Chicago CBD. The population increase along this path was bimodal, with no notable increase along the middle of the track, bounded by a large increase in both population (Fig. 2b) and housing units (not shown) due to suburban development near the first third of the track and urban-core, high-rise residential development near the tornado's terminus. The latter, CBD-focused increase in population and housing units is a recent reversal in long-term development trends found in many cities (Census Bureau 2012b). While suburbanization and exurbanization has continued in the past decade, a secondary, focused ''inward migration'' has taken place as more jobs in and near the CBD have attracted more residents desiring to move downtown that, in turn, becomes a magnet for more employers (Ehrenhalt 2013). From 2001 to 2010, Chicago underwent the largest numeric and percentage gain in its downtown area of any of the largest cities in the United States (Census Bureau 2012b). This demographic transformation illustrates how the continually evolving spatiotemporal character of development can dramatically

influence the disaster potential landscape, especially at the microscale.

Scenarios P2 and P3 tracked across locales that have witnessed growth, but not of the magnitude found along the city's more focused ring of development located approximately 60–80 km from the CBD (Greene and Pick 2013). Nevertheless, the development found near the origin of these paths still leads to 15%–22% increases in exposure metrics during this two-decade period for the scenarios.

2) 10-KM SYNTHETIC SCENARIOS

Using a synthetic's entire path length (e.g., 45–67 km; Table 2) leads to scenarios where the damage footprint inevitably stretches across multiple development types, causing difficulty in evaluating specific land-use change effects on disaster potential. To generate a more focused analysis of how development has influenced disaster potential, we use a 10-km segment of the synthetic S2 (Fig. 2c) to target specific land use types and their changes from 1990 to 2010. As discussed in section 3c, the 10-km segment we use is representative of a tornado striking a developed region.

First, we placed the 10-km S2 segment across particular development types to assess changes in exposure where the land use has been relatively constant over the 20-yr period as determined by an evaluation of land-use data derived from the three decennial censuses (e.g., Fig. 2c). This promotes an evaluation of how *each* of the differing land use types is contributing to the overall change in tornado exposure (Table 10).

Both urban tornado scenarios, Ur1 and Ur2, experienced losses in population, reconfirming the slow exodus of people from the immediate area surrounding the CBD. The near-central city of Chicago, as with most large cities in the Midwest and Northeast, has been defined by perennial population declines (excluding a small expansion in the 1990s) since the 1950s (Greene and Pick 2012). These declines are due to the abandonment of the area immediately around the urban core by the middle class, giving rise to an urban underclass characterized by little upward mobility that results in poor neighborhoods, high crime rates, and diminished amenities (Wilson 1987, 1996; Hudson 2006; Greene and Pick 2012). Whereas the exposure in these areas may be stable or have decreased during the period examined, other components of vulnerability may have changed that could result in far greater disaster potential. Conceptually, vulnerability can be differentiated by three constituents: exposure (characteristics of the natural and/or built environment that position a system to be affected by a hazard; in this study, people and their housing units), sensitivity/susceptibility (the degree to which a system is affected by hazard conditions), and adaptive capacity (ability for the system to cope or adapt to hazard conditions) (Adger 2006; Polsky et al. 2007; Morss et al. 2011; Fekete 2012). We have employed a disintegrative methodology that examines a distinct component of vulnerability (exposure), which we argue promotes a more measured and quantified analysis of that element. However, this singular analysis does not permit the discovery of how important the other constituents of vulnerability are, and how they integrate with one another, in these particular cases. For instance, in areas that have witnessed urban decay, people would arguably have increased susceptibility and decreased adaptive capacity to disasters that could lead to far greater disaster consequences (Wisner et al. 2004; Paul 2011).

Scenario segments in the suburban locations, Su1 and Su2, generated mixed results. Changes in affected population in the segments were negligible, with both areas experiencing increases in housing units. These areas of DuPage (Su1) and Cook (Su2) Counties were developed largely prior to the period of analysis (Fig. 2d), with only limited, fill-in development increasing the housing unit metric. Of the segment scenarios placed over temporally consistent land-use types, exurban scenario Ex1 underwent the greatest amplification in exposure magnitude. The area of central Kane County has continued to see development, with much of the area already, or on the cusp of, converting from exurban to suburban classification. Therefore, even in low-density developed areas, there has been a continued escalation in density and, thus, exposure. Uniquely, scenario Ex2 witnessed a notable drop in population exposure, with a near 20% increase in housing units, with much of that increase occurring during the 1990–2000 period. Both exposure measurements for the two rural cases examined, Ru1 and Ru2, decreased. Although rural population loss is endemic to many rural areas in the United States (McGranahan and Beale 2002), the decreases found here must be deciphered with caution. The decreases in population are on the order of a couple dozen, with housing unit losses sometimes less than 1 unit per scenario. In comparison to the exposure values found for urban, suburban, and even exurban areas, these impacted numbers are very small.

Next, five track segments were placed explicitly across locations where kernel density estimation analyses (not shown) on land-use change data (e.g., Fig. 2d) revealed clusters of grid cells that underwent rural-to-exurban or exurban-to-suburban change (Table 10). This analysis targets how low- and high-density sprawl has contributed to the overall disaster potential picture. Track segments T1 and T2 are represented by areas that transitioned from rural to exurban land use classifications. Both T1 and T2

TABLE 10. Number of people and housing units affected and affiliated 1990–2010 percentage changes of total impacted for simulated 10-km tornado segments across Chicago region based on the S2 scenario (cf. Figs. 2c,d). Counts for those areas affected by significant (EF2+) and violent (EF4+) damage are also provided.

		Population				Housing units			
Position	Year	EF2-EF5	EF4-EF5	EF0-EF5	1990–2010 % change	EF2-EF5	EF4-EF5	EF0-EF5	1990–2010 % change
Ur1	1990	48 104	18 424	115 971		19 500	7089	49 575	
	2000	47 643	18 487	115 881		21 245	7961	53 473	
	2010	44 705	17 392	111 419	−3.9%	23 491	9017	60 171	21.4%
Ur2	1990	35 505	13 527	91 753		13 895	5302	35 497	
	2000	33 908	12 939	87 094		13 211	5021	33 744	
	2010	27 001	10 299	70 006	−23.7%	12 983	4963	32 927	−7.2%
Su1	1990	8471	3238	22 288		3152	1209	7848	
	2000	8154	3010	22 556		3031	1149	7812	
	2010	8288	3097	22 388	0.4%	3201	1216	8066	2.8%
Su2	1990	5999	2270	16 568		1896	715	5357	
	2000	5960	2231	17 120		1979	744	5868	
	2010	5951	2303	16 155	−2.5%	2180	841	6138	14.6%
Ex1	1990	958	375	2365		283	111	704	
	2000	1267	486	3306		379	145	989	
	2010	1360	519	3595	52.0%	447	171	1181	67.7%
Ex2	1990	124	47	366		39	15	114	
	2000	126	48	385		46	18	139	
	2010	112	43	341	−6.8%	46	18	136	19.7%
Ru1	1990	26	10	68		9	3	23	
	2000	24	9	64		9	3	23	
	2010	19	7	51	−24.6%	9	3	23	−1.6%
Ru2	1990	23	9	65		8	3	22	
	2000	18	7	49		7	3	18	
	2010	15	6	41	−36.8%	7	3	19	−15.7%
T1	1990	61	24	173		20	8	57	
	2000	111	43	329		37	14	108	
	2010	241	93	626	261.2%	82	32	211	271.6%
T2	1990	62	23	175		22	8	61	
	2000	91	39	211		32	13	75	
	2010	69	26	188	7.3%	26	10	73	19.9%
T3	1990	1540	591	4,367		578	221	1628	
	2000	8008	3067	21 058		2585	986	6912	
	2010	9374	3638	23 900	447.3%	3098	1200	8108	398.0%
T4	1990	3163	1325	7045		1061	443	2363	
	2000	6724	2703	14 620		2137	865	4730	
	2010	8624	3424	19 814	181.2%	2805	1119	6596	179.1%
T5	1990	388	123	2377		150	48	863	
	2000	2603	960	8576		879	325	2816	
	2010	4888	1917	13 394	463.5%	1700	667	4518	423.6%

track segments illustrate positive percentage changes in population and housing units impacted from 1990 to 2010, although results are tempered by the low affected counts. The amplification in tornado exposure for the T1 and T2 segments is due to increased development and affiliated sprawl apparent in these areas over the past two decades. Areas that were once largely row-crop farmland have since transitioned to exurban development, incrementally increasing hazard targets and the expanding bull's-eye effect. Tornado scenario segments T3, T4, and T5 are characterized by areas that have transitioned from exurban to suburban land use classifications. All three of these tornado scenario segments exemplify extremely large (>150%) positive percent increases in population and housing units impacted from 1990 to 2010. Indeed, these segments contain collectively the largest percentage increases found in any of the segment scenarios suggesting that it is this particular development change that has led to the greatest expansion in the exposure to weather hazards in this region.

5. Discussion and conclusions

We have employed the contextual argument that exposure is a "condition *sine qua non* for disaster risk to exist" (UNDP 2004). Moreover, population growth is not

spatially uniform and, therefore, exposure is not distributed evenly across the landscape. For instance, cities and suburbs grow directionally and, consequently, the evaluation of the spatial character of exposure is as important as other interrogatives. Because of data, computational, and methodological restrictions, research quantifying *changes* in hazard exposure has been relatively limited. Using conventional spatiotemporal change methods on standard, relatively large, enumeration units, previous works (e.g., Hall and Ashley 2008; Paulikas and Ashley 2011) have investigated shifts in weather-related exposure at the metropolitan scale. These methods lacked the sophistication necessary to assess a spectrum of geographic extents and generate more substantial conclusions regarding exposure's culpability in augmenting tornado disaster consequences. Preceding evaluations of exposure tend to aggregate at spatial extents far larger than the hazard footprint, especially for microscale hazards spawned by severe thunderstorms. The incongruence of spatial scales of analysis often precluded an assessment of the relationship between the underlying constituents requisite for disaster. This investigation offered an initial step toward rectifying these perceived deficiencies, fostering a homogenized approach for assessing and quantifying changes in finescale weather hazard exposure and providing a framework for future work exploring exposure and vulnerability's contribution to disasters.

Specifically, through a geographic lens, we assessed how an increasing and spreading population is leading to substantial growth in tornado hazard exposure rates, appearing to offset, or counteract, contemporary scientific and technological advances in mitigation (e.g., warning systems, Doppler radar, etc.) as exemplified in recent tornado disasters. We employed spatial data modeling and spatial analytic approaches that appraised contemporary changes in the relationship between tornadoes and the distribution of people and their residences for the case of Chicago. Results proved that, generally, the number of people and their housing continues to grow and geographically expand, promoting an increasing hazard target, or what we termed the expanding bull's-eye effect. Metropolitan-scale assessments of Chicago's demographic, housing unit, and land-use types confirm that, simply, more people and their possessions are in the potential path of tornadoes. This finding is not entirely unexpected, but we illustrate specifically how differing development types lead to varying exposure rates that contribute to the unevenness of potential weather-related disasters across the landscape. For instance, suburbanization development character associated with high-density sprawl has led to the greatest change in exposure landscape in the Chicago area. Conversely, along the periphery of the urban core, long-term population loss has led to decreasing amounts of people to be affected; however, those that remain may be highly vulnerable due to enhanced sensitivity/susceptibility and reduced adaptive capacity (e.g., see Klinenberg 2002)—components of vulnerability we did not examine in this study. More recently, inward migration to CBDs (Census Bureau 2012b; Ehrenhalt 2013) has promoted a very dense exposure in the urban core with concentrated catastrophic disaster potential that could potentially overwhelm the critical infrastructure sectors (Homeland Security 2009) of most, if not all, cities, including Chicago.

A simple conceptual model (Fig. 4) is provided to illustrate how spatiotemporal development changes found in metropolitan regions have led to and will continue to foster an expanding bull's-eye effect, placing ever increasing amounts of ''targets''—people, built environments, and infrastructure—in harm's way of tornadoes and other geophysical and technical hazards. We have argued it is not solely the population magnitude that is important in creating disaster potential; rather, it is how the population, and its affiliated built environment, is distributed across the geographical landscape that defines how the fundamental components of risk and vulnerability are realized in a disaster. The model proposed reveals the broad concept of the expanding bull's-eye effect with the inferred understanding that each city and/or regional development footprint will be constrained by a diverse set of social, economic (Hardaway 2011), political (e.g., land-use planning, park designation, etc.), and physical (e.g., Lake Michigan in Chicago's case) elements.

In addition, our research appraised the viability of using a gridded framework for assessing the changes in census-derived exposure data. The gridded methodology removes the spatial unit variation problem found when using two or more census time stamps (Cai et al. 2006) and promotes an evaluation of temporal changes in the underlying vulnerability, a dimension often excluded from exposure studies. Results revealed that the modifiable unit problem (MAUP; Openshaw 1984) was still influential. MAUP occurs when spatial aggregations of data (e.g., changing census enumerations, differing grid resolutions) lead to dissimilar results, a prevalent analysis obstacle in studies employing spatial enumerations of aggregated data (Mennis 2002; Holt et al. 2004; Cai et al. 2006). The difference between gridded county-, tract-, and block-level data in the estimation of potentially affected exposure units by the same tornado scenario exemplifies the effect of different areal unit sizes (Tables 6 and 7). Since tornadoes have relatively small hazard footprints, the finest analysis resolution provides the most precise results (Schlossberg 2003).

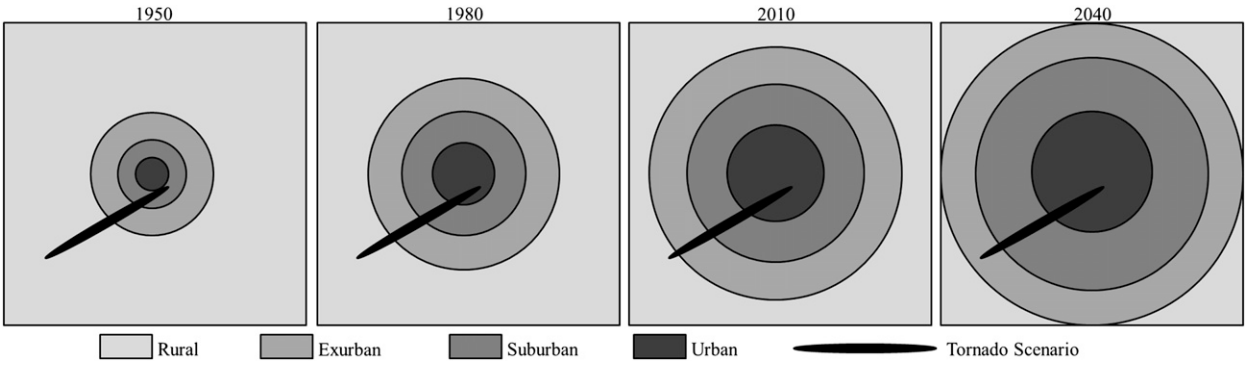

FIG. 4. A conceptual model of the expanding bull's-eye effect for a hypothetical metropolitan region that is characterized by increasing development spreading from an urban core over time. A sample tornado scenario is overlaid to show how expanding development creates larger areas of potential impacts from hazards.

The investigation also assed tornado dimensions employed in previous scenario-based research. An analysis of historical significant and violent tornado events found that the high-end width scenarios in WUR are not likely representative of even the most extreme potential tornadoes. We offer a structure for synthetic development based on observed damage indicators for a modern catastrophic event (2011 Joplin EF5). This methodology promoted a flexible, yet observationally constrained framework for developing tornado synthetics that can be used in models to assess potential social, physical, and economic losses from tornadoes. Additional work conflating damage indictors, mobile Doppler radar data, and in situ observations is required to build a more robust and realistic tornado scenario model.

While climate change *may* amplify the risk of certain hazards,[2] the root cause of escalating disasters is not necessarily event frequency, or risk, related. Rather, as affirmed by previous research (e.g., Changnon et al. 2000; Cutter 2010; Bouwer 2011; Barthel and Neumayer 2012; Simmons et al. 2013) and illustrated herein, the growing trend in disasters is likely due to 1) the increasing density and spread of humans and property in harm's way, or exposure, and 2) the increasing vulnerability of the population. We have focused explicitly on the physical exposure components of population and their residences to tornadoes in the third largest metropolitan area in the United States—a region that has a relatively elevated risk of tornado risk (Brooks et al. 2003). This research methodology could be replicated across a variety of spatiotemporal domains, as well as for other hazards. Recent tornado catastrophes (e.g., the 27–28 April 2011 tornado outbreak, 22 May 2011 Joplin tornado, 20 May 2013 Moore, etc.) reveal that there is much to be learned about how hazards interact with society and, perhaps more importantly, how society interacts with hazards. Studies engaging a worst-case hazard scenario approach using representative hazard models on high-spatial-resolution datasets of historical or forecast vulnerability constituents could spur mitigation activities and policy changes with the goal of reducing hazard impacts. An essential part of that research must focus on understanding how the exposure landscape has transformed over time and how those spatiotemporal changes may influence the tasks of warning, rescue, and recovery should a catastrophic scenarios come to fruition. Discovered spatiotemporal trends of hazard exposure will assist policy makers, hazard scientists, and the public by illustrating the role amplifying exposure has on the increasing hazard impacts.

Acknowledgments. The authors wish to thank Mr. Tim Marshall (Haag Engineering) for supplying detailed maps of his Joplin tornado damage survey. The authors appreciate critical comments and productive discussions provided by Drs. David Changnon and Richard Greene (NIU). We also thank the efforts of Mr. Donald Heins (NIU alumnus), who assisted in the development of early versions of the GIS gridding routine. Finally, we appreciate the thoughtful reviews provided by the anonymous referees.

[2] Research evaluating the potential impacts from large-scale effects of teleconnections and/or climate change due to anthropogenically enhanced global radiative forcing on microscale thunderstorm hazard risk is in its infancy and, currently, inconclusive (Brooks 2013; Kunkel et al. 2013).

REFERENCES

Adger, W. N., 2006: Vulnerability. *Global Environ. Change,* **16,** 268–281.

Ashley, W. S., 2007: Spatial and temporal analysis of tornado fatalities in the United States: 1880–2005. *Wea. Forecasting,* **22,** 1214–1228.

Auch, R., J. Taylor, and W. Acevedo, 2004: Urban growth in American cities: Glimpses of U.S. urbanization. Circular 1252,

U.S. Department of the Interior, U.S. Geological Survey, 52 pp. [Available online at http://pubs.usgs.gov/circ/2004/circ1252/.]

Balk, D., M. Brickman, B. Anderson, F. Pozzi, and G. Yetman, 2005: Mapping global urban and rural population distributions: Estimates of future global population distribution to 2015. Center for International Earth Science Information Network, Socioeconomic Data and Applications Center, Columbia University, 77 pp. [Available online at http://sedac.ciesin.columbia.edu/gpw/docs/GISn.24_web_gpwAnnex.pdf.]

Barthel, F., and E. Neumayer, 2012: A trend analysis of normalized insured damage from natural disasters. *Climatic Change,* **113,** 215–237.

Blumenfeld, K., 2008: Comments on ''Low-level winds in tornadoes and potential catastrophic tornado impacts in urban areas.'' *Bull. Amer. Meteor. Soc.,* **89,** 1578–1579.

Bouwer, L. M., 2011: Have disaster losses increased due to anthropogenic climate change? *Bull. Amer. Meteor. Soc.,* **92,** 39–46.

Brooks, H. E., 2004: On the relationship of tornado path length and width to intensity. *Wea. Forecasting,* **19,** 310–319.

——, 2013: Severe thunderstorms and climate change. *Atmos. Res.,* **123,** 129–138, doi:10.1016/j.atmosres.2012.04.002.

——, C. A. Doswell III, and M. P. Kay, 2003: Climatological estimates of local daily tornado probability. *Wea. Forecasting,* **18,** 626–640.

——, ——, and D. Sutter, 2008: Comments on ''Low-level winds in tornadoes and potential catastrophic tornado impacts in urban areas.'' *Bull. Amer. Meteor. Soc.,* **89,** 87–90.

Burkett, V. R., and M. A. Davidson, 2012: Coastal impacts, adaptation and vulnerability: A technical input to the 2012 National Climate Assessment. Cooperative Report to the 2013 National Climate Assessment, 150 pp. [Available online at http://www.coastalstates.org/wp-content/uploads/2011/03/Coastal-Impacts-Adaptation-Vulnerabilities-Oct-2012.pdf.]

Burton, C., 2010: Social vulnerability and hurricane impact modeling. *Nat. Hazards Rev.,* **11,** 58–68.

Cai, Q., G. Rushton, B. Bhaduri, E. Bright, and P. Coleman, 2006: Estimating small-area populations by age and sex using spatial interpolation and statistical inference methods. *Trans. GIS,* **10,** 577–598.

Census Bureau, 1994: Geographic Areas Reference Manual (GARM). Department of Commerce, United States Census Bureau. [Available online at http://www.census.gov/geo/reference/garm.html.]

——, cited 2012a: Growth in urban population outpaces rest of nation. Department of Commerce, United States Census Bureau. [Available online at http://www.census.gov/newsroom/releases/archives/2010_census/cb12-50.html.]

——, cited 2012b: Populations increasing in many downtowns. Department of Commerce, United States Census Bureau. [Available online at http://www.census.gov/newsroom/releases/archives/2010_census/cb12-181.html.]

Changnon, S. A., and J. Burroughs, 2003: The tristate hailstorm: The most costly on record. *Mon. Wea. Rev.,* **131,** 1734–1739.

——, R. A. Pielke Jr., D. Changnon, R. T. Sylves, and R. Pulwarty, 2000: Human factors explain the increased losses from weather and climate extremes. *Bull. Amer. Meteor. Soc.,* **81,** 437–442.

Clarke, L., 2005: Worst-case thinking: An idea whose time has come. *Nat. Hazards Obs.,* **293,** 1–3.

Cutter, S. L., 2010: Social science perspectives on hazards and vulnerability science. *Geophysical Hazards: Minimizing Risk, Maximizing Awareness,* T. Beer, Ed., Springer Netherlands, 17–30.

Deichmann, U., D. Balk, and G. Yetman, 2001: Transforming population data for interdisciplinary usages: From census to grid. Center for International Earth Science Information Network, Socioeconomic Data and Applications Center, Columbia University. 19 pp. [Available online at http://sedac.ciesin.columbia.edu/gpw-v2/GPWdocumentation.pdf.]

Dell'Acqua, F., P. Gamba, and K. Jaiswal, 2013: Spatial aspects of building and population exposure data and their implications for global earthquake exposure modeling. *Nat. Hazards,* **68,** 1291–1309, doi:10.1007/s11069-012-0241-2.

Doswell, C. A., III, H. E. Brooks, and N. Dotzek, 2009: On the implementation of the Enhanced Fujita scale in the USA. *Atmos. Res.,* **93,** 554–563.

Duany, A., E. Plater-Zyberk, and J. Speck, 2000: *Suburban Nation: The Rise of Sprawl and the Decline of the American Dream.* North Point Press, 320 pp.

Ehrenhalt, A., 2013: *The Great Inversion and the Future of the American City.* Vintage, 288 pp.

Fekete, A., 2012: Spatial disaster vulnerability and risk assessments: Challenges in their quality and acceptance. *Nat. Hazards,* **61,** 1161–1178.

Field C. B., and Coauthors, Eds., 2012: *Managing the Risks of Extreme Events and Disasters to Advance Climate Change Adaptation.* Cambridge University Press, 582 pp.

Gillham, O., 2002: *The Limitless City: A Primer on the Urban Sprawl Debate.* Island Press, 309 pp.

Greene, R. P., and J. B. Pick, 2012: *Exploring the Urban Community: A GIS Approach.* 2nd ed. Prentice Hall, 432 pp.

——, and ——, 2013: Shifting patterns of suburban dominance: The case of Chicago from 2000 to 2010. *J. Maps,* **9,** 178–182.

Hall, S. G., and W. S. Ashley, 2008: The effects of urban sprawl on the vulnerability to a significant tornado impact in northeastern Illinois. *Nat. Hazards Rev.,* **9,** 209–219.

Hardaway, R. M., 2011: *The Great American Housing Bubble: The Road to Collapse.* Praeger, 256 pp.

Holt, J. B., C. P. Lo, and T. W. Hodler, 2004: Dasymetric estimation of population density areal interpolation of census data. *Cartogr. Geogr. Inf. Sci.,* **31,** 101–121.

Homeland Security, 2009: *National Infrastructure Protection Plan.* United States Department of Homeland Security, 175 pp. [Available online at http://www.dhs.gov/xlibrary/assets/NIPP_Plan.pdf.]

Höppe, P., and R. A. Pielke Jr., 2006: Workshop on Climate Change and Disaster Losses: Understanding and attributing trends and projections. Final Workshop Report, 266 pp. [Available online at http://cstpr.colorado.edu/sparc/research/projects/extreme_events/munich_workshop/full_workshop_report.pdf.]

Hudson, J., 2006: *Chicago: A Geography of the City and Its Region.* University of Chicago Press, 356 pp.

Kahn, S., and I. Kelman, 2012: Progressive Climate Change and Disaster Losses: Connections and metrics. *Nat. Hazards,* **61,** 1477–1481.

Klinenberg, E., 2002: *Heat Wave: A Social Autopsy of Disaster in Chicago.* University of Chicago Press, 320 pp.

Kunkel, K. E., R. A. Pielke, and S. A. Changnon, 1999: Temporal fluctuations in weather and climate extremes that cause economic and human health impacts: A review. *Bull. Amer. Meteor. Soc.,* **80,** 1077–1098.

——, and Coauthors, 2013: Monitoring and understanding trends in extreme storms: State of knowledge. *Bull. Amer. Meteor. Soc.,* **94,** 499–514.

Lemon, L. R., and M. Umscheid, 2008: The Greensburg, Kansas, tornadic storm: A storm of extremes. Preprints, *24th Conf. on Severe Local Storms,* Savannah, GA, Amer. Meteor. Soc., P2.4. [Available online at http://ams.confex.com/ams/pdfpapers/141811.pdf.]

Lerner-Lam, A., 2007: Assessing global exposure to natural hazards: Progress and future trends. *Environ. Hazards,* **7,** 10–19.

Marshall, T. P., W. Davis, and S. Runnels, 2012: Damage survey of the Joplin tornado. Preprints, *26th Conf. on Severe Local Storms,* Nashville, TN, Amer. Meteor. Soc., 6.1. [Available online at https://ams.confex.com/ams/26SLS/webprogram/Manuscript/Paper211662/Joplinmerger.pdf.]

McCarthy, D., and J. Schaefer, 2005: 2004 year in tornadoes: What a year it was! *Extended Abstracts, 34th Conf. on Broadcast Meteorology,* Washington, DC, Amer. Meteor. Soc., 2.1. [Available online at https://ams.confex.com/ams/WAFNWP34BC/techprogram/paper_95244.htm.]

McDonald, J., and K. C. Mehta, 2006: A recommendation for an Enhanced Fujita scale (EF-Scale). Wind Science and Engineering Center, Texas Tech University, 111 pp. [Available online at http://www.depts.ttu.edu/nwi/Pubs/FScale/EFScale.pdf.]

McGranahan, D. A., and C. L. Beale, 2002: Understanding rural population loss. *Rural Amer.,* **17** (4), 2–11. [Available online at www.ers.usda.gov/publications/ruralamerica/ra174/ra174a.pdf.]

Mennis, J., 2002: Using geographic information systems to create and analyze statistical surfaces of population and risk for environmental justice analysis. *Soc. Sci. Quart.,* **83,** 281–297.

——, 2009: Dasymetric mapping for estimating population in small areas. *Geogr. Compass,* **3,** 727–745.

Morss, R., O. Wilhelmi, G. A. Meehl, and L. Dilling, 2011: Improving societal outcomes of extreme weather in a changing climate: An integrated perspective. *Annu. Rev. Environ. Resour.,* **36,** 1–25.

Nicholls, N., 2001: Atmospheric and climatic hazards: Improved monitoring and prediction for disaster mitigation. *Nat. Hazards,* **23,** 137–155.

——, 2011: Comments on ''Have disaster losses increased due to anthropogenic climate change?'' *Bull. Amer. Meteor. Soc.,* **92,** 791.

Nicholls, R. J., and C. Small, 2002: Improved estimates of coastal population and exposure to hazards released. *Eos, Trans. Amer. Geophys. Union,* **83,** 301–305, doi:10.1029/2002EO000216.

NWS, 2011: Joplin tornado event summary. Springfield, MO, Weather Forecast Office. [Available online at http://www.crh.noaa.gov/sgf/?n=event_2011may22_summary.]

Openshaw, S., 1984: *The Modifiable Areal Unit Problem.* Concepts and Techniques in Modern Geography Series, Vol. 38, Geo Books, 41 pp. [Available online at http://qmrg.org.uk/files/2008/11/38-maup-openshaw.pdf.]

Paul, B. K., 2011: *Environmental Hazards and Disasters.* John Wiley and Sons, 322 pp.

Paulikas, M. J., and W. S. Ashley, 2011: Thunderstorm hazard vulnerability for the Atlanta, Georgia metropolitan region. *Nat. Hazards,* **58,** 1077–1092.

Peduzzi, P., B. Chantenoux, H. Dao, A. De Bono, C. Herold, J. Kossin, F. Mouton, and O. Nordbeck, 2012: Global trends in tropical cyclone risk. *Nat. Climate Change,* **2,** 289–294.

Pielke, R. A., Jr., 2005: Attribution of disaster losses. *Science,* **311,** 1615–1616.

——, 2007: Future economic damage from tropical cyclones: Sensitivities to societal and climate changes. *Philos. Trans. Roy. Soc. London,* **365A,** 2717–2729.

Pinelli, J.-P., E. Simiu, K. Gurley, C. Subramanian, L. Zhang, A. Cope, J. Filliben, and S. Hamid, 2004: Hurricane damage prediction model for residential structures. *J. Struct. Eng.,* **130,** 1685–1691.

Polsky, C., R. Neff, and B. Yarnal, 2007: Building comparable global change vulnerability assessments: The vulnerability scoping diagram. *Global Environ. Change,* **17,** 472–485.

Rae, S., and J. Stefkovich, 2000: The tornado damage risk assessment predicting the impact of a big outbreak in Dallas–Fort Worth, Texas. *Extended Abstracts, 20th Conf. on Severe Local Storms,* Orlando, FL, Amer. Meteor. Soc., 9.6. [Available online at https://ams.confex.com/ams/Sept2000/techprogram/paper_16405.htm.]

Remo, J. W. F., and N. Pinter, 2012: Hazus-MH earthquake modeling in the central USA. *Nat. Hazards,* **63,** 1055–1081.

——, M. Larson, and N. Pinter, 2012: Hydraulic and flood-loss modeling of levee, floodplain, and river management strategies, middle Mississippi River, USA. *Nat. Hazards,* **61,** 551–575.

Scawthorn, C., P. Schneider, and B. Schauer, 2006: Natural hazards—The multihazard approach. *Nat. Hazards Rev.,* **7,** 39.

Schlossberg, M., 2003: GIS, the US Census and neighbourhood scale analysis. *Plann. Pract. Res.,* **18,** 213–217.

SEDAC, cited 2011: U.S. Census grids. Socioeconomic Data and Applications Center, Columbia University. [Available online at http://sedac.ciesin.columbia.edu/usgrid/.]

Simmons, K. M., and D. Sutter, 2011: *The Economic and Societal Impact of Tornadoes.* University of Chicago Press, 282 pp.

——, ——, and R. Pielke Jr., 2013: Normalized tornado damage in the United States: 1950–2011. *Environ. Hazards,* **12,** 132–147.

Speheger, D. A., C. A. Doswell III, and G. J. Stumpf, 2002: The tornadoes of 3 May 1999: Event verification in central Oklahoma and related issues. *Wea. Forecasting,* **17,** 362–381.

Suckling, P. W., and W. S. Ashley, 2006: Spatial and temporal characteristics of tornado path direction. *Prof. Geogr.,* **58,** 20–38.

Theobald, D. M., 2005: Landscape patterns of exurban growth in the USA from 1980 to 2020. *Ecol. Soc.,* **10** (32). [Available online at http://www.ecologyandsociety.org/vol10/iss1/art32/.]

Trenberth, K., A. Watson, R. A. Pielke Jr., K. Emanuel, J. Curry, L. Bouwer, G. C. Hegerl, and W. Hooke, cited 2011: Forum: Is extreme weather linked to global warming? *Yale Environ. 360,* 2 June 2011. [Available online at http://e360.yale.edu/feature/forum_is_extreme_weather_linked_to_global_warming/2411/.]

UNDP, 2004: Reducing disaster risk: A challenge for development. M. Pelling et al., Eds., United Nations Development Programme, Bureau for Crisis Prevention and Recovery, 146 pp. [Available online at http://www.undp.org/content/dam/undp/library/crisis%20prevention/disaster/asia_pacific/Reducing%20Disaster%20risk%20a%20Challenge%20for%20development.pdf.]

Wilson, S. G., and T. R. Fischetti, 2010: Coastline population trends in the United States: 1960 to 2008. U.S. Census Bureau, P25-1139, 27 pp. [Available online at http://www.census.gov/prod/2010pubs/p25-1139.pdf.]

Wilson, W. J., 1987: *The Truly Disadvantaged: The Inner City, the Underclass and Public Policy.* University of Chicago Press, 320 pp.

——, 1996: *When Work Disappears: The World of the New Urban Poor.* Knopf, 322 pp.

Wisner, B., P. Blaikie, T. Cannon, and I. Davis, 2004: *At Risk: Natural Hazards, People's Vulnerability, and Disasters.* 2nd ed. Routledge, 496 pp.

Wu, S., X. Qiu, and L. Wang, 2005: Population estimation methods in GIS and remote sensing: A review. *GIScience Remote Sens.,* **42,** 80–96.

Wurman, J., and C. Alexander, 2005: The 30 May 1998 Spencer, South Dakota, storm. Part II: Comparison of observed damage and radar-derived winds in the tornadoes. *Mon. Wea. Rev.,* **133,** 97–119.

——, ——, P. Robinson, and Y. Richardson, 2007: Low-level winds in tornadoes and potential catastrophic tornado impacts in urban areas. *Bull. Amer. Meteor. Soc.,* **88,** 31–46.

——, ——, ——, and ——, 2008: Reply. *Bull. Amer. Meteor. Soc.,* **89,** 90–94.

Yuan, M., M. Dickens-Micozzi, and M. A. Magsig, 2002: Analysis of tornado damage tracks from the 3 May tornado outbreak using multispectral satellite imagery. *Wea. Forecasting,* **17,** 382–398.